

Journal of Biomedical Optics

SPIDigitalLibrary.org/jbo

Targeted microinjection into cells and retina using optoporation

Ling Gu
Samarendra K. Mohanty

Targeted microinjection into cells and retina using optoporation

Ling Gu and Samarendra K. Mohanty

University of Texas at Arlington, Department of Physics, Biophysics and Physiology Lab, Arlington, Texas 76019

Abstract. The laser microbeam has enabled highly precise noncontact delivery of exogenous materials into targeted cells without compromising cell viability, which has been a highly challenging task for traditional methods. Here, we report targeted delivery of impermeable substances into mammalian cells and goldfish retinal explants subsequent to ultrafast laser microbeam assisted injection. Introduction of impermeable dye into the cell through localized pore formation was confirmed by distinct fluorescence at the site of pore formation on the membrane and its spatiotemporal diffusion pattern through the nucleus. Indirect optoporation by bubble formation, external to cell, led to a similar spatial diffusion pattern but with a larger time constant for injection. Using optimized laser intensity, exposure, and a spatial irradiation pattern, desired spatial transfection patterns in goldfish retina explants were achieved as confirmed by the expression of injected plasmids encoded for light-activable channelrhodopsin-2 ion-channel, tagged with fluorescent protein. Laser assisted delivery of exogenous material into a specific area of three-dimensional neuronal tissue, such as the retina, will help to understand the functioning of neuronal circuitry of normal and degenerated retina. © 2011 Society of Photo-Optical Instrumentation Engineers (SPIE). [DOI: 10.1117/1.3662887]

Keywords: optoporation; laser microbeam; ultrafast laser; laserfection; ChR2-YFP; retinal neurons.

Paper 11260PRR received May 24, 2011; revised manuscript received Oct. 22, 2011; accepted for publication Nov. 1, 2011; published online Dec. 6, 2011.

1 Introduction

Introduction of foreign DNA and fluorescent compounds into intact cells is essential for a variety of applications in cell biology, such as visualization of specific structures, genetic manipulation, and functional alterations. While conventional physical techniques such as microinjection using thin glass capillaries or microelectroporation are invasive and tedious, chemical methods including viral transfection and lipofection are not specific to a single cell in a monolayer cell culture or in a three-dimensional tissue. Further, transfection efficiency of these methods varies depending on the cell type and handling procedure. In last 2 decades, laser-assisted poration has been utilized to efficiently introduce macromolecular substances into intact cells. By using a tightly focused laser beam, the cell membrane can be perforated in a highly controlled manner, allowing exogenous molecules to enter the cell. Since a diffraction-limited spot size of a UV laser beam is smaller and absorption of the cell membrane is high in the UV-band, lasers in this spectral range were the first to be used for microinjection.¹ However, UV light raises the potential of collateral damage to cellular components or even to the foreign DNA being transferred into cells;¹ therefore the use of UV light may not be suitable for noninvasive microinjection. The continuous-wave argon-ion laser operating at 488 nm (Refs. 2 and 3) and frequency-doubled Nd:YAG laser operating at 532 nm (Ref. 4) have also been employed for optoporation. However, since several cellular components have a significant absorption at these wavelengths, the pos-

sibility of detrimental effects at these wavelengths cannot be ruled out. Owing to the fact that absorption of cellular components are least in the near-infrared (NIR) biological window of 700 to 1000 nm,⁵⁻⁸ a NIR ultrafast laser beam has been employed for laser-assisted poration. Because of highly localized damage by nonlinear optical absorption which fades away significantly for out-of-focus cellular components, a femtosecond laser beam could microinject exogenous genes into cells with very high efficiency.⁹⁻¹¹ The ultrahigh-intensity as it exists in a tightly-focused femtosecond-pulsed laser beam resulted in the formation of a site-specific, transient perforation,⁹ more precisely than a nanosecond-pulsed laser beam.⁵ However, it has been highly challenging to carry out microinjection into fragile cells including primary neurons. Further, to the best of our knowledge, the femtosecond laser microbeam has not been utilized for transfection of a three-dimensional neuronal tissue.

In this study, we employed a femtosecond NIR Ti:Sapphire laser for optoporation of impermeable dye into two mammalian cell types, i. human intrahepatic biliary epithelial cells (HI-BEC) and ii. human fibrosarcoma cells HT1080. We found that though exogenous impermeable dye could be injected by laser from specific sites on the cell membrane either by i. direct pore formation or ii. extracellular bubble formation, the kinetics of injection is significantly different. Moreover, using optimized laser intensity, exposure, and a spatial irradiation pattern, the desired spatial transfection patterns in goldfish retina explants could be achieved by injection of plasmids encoded for light-activable channelrhodopsin-2 (ChR2), tagged with fluorescent protein.

Address all correspondence to: Samarendra Mohanty, University of Texas at Arlington, Department of Physics, Biophysics and Physiology Group, 502 Yates Street, 108 Science Hall, Arlington, Texas 76019; Tel. 817-272-1177; Fax: +1-817-272-3637; E-mail smohanty@uta.edu.

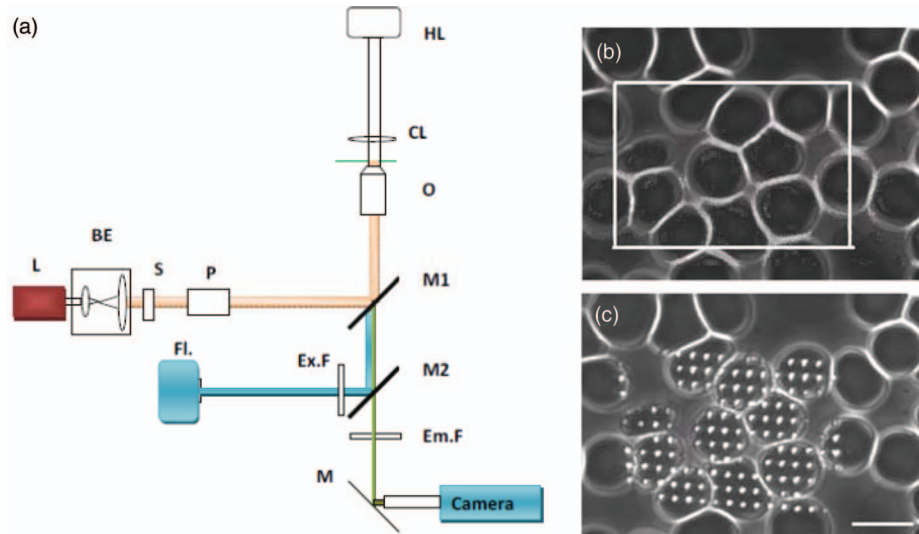


Fig. 1 (a) Experimental setup for femtosecond laser-assisted optoporation. L: Ti: Sapphire laser; BE: beam expander; S: uniblitz shutter; P: polarizer; Fl.: fluorescence excitation source; Ex: excitation filter; Em: emission filter; MO: microscope objective; CL: condenser lens; DM1 and DM2: dichroic mirrors; M: mirror; HL: halogen lamp. Red blood cells before (b) and after (c) patterned ultrafast laser microbeam irradiation.

2 Materials and Methods

2.1 Cell Culture

HIBEC and HT1080 cells were routinely cultured in Dulbecco's modified Eagle's medium (DMEM) supplemented with 10% fetal bovine serum. For laser-assisted microinjection of propidium iodide (PI), cells were trypsinized and plated on poly-D-lysine-coated cover slips. The cultures were maintained at 37°C in a 5% CO₂ humidified atmosphere. Red blood cells (RBCs) of healthy volunteers were also used for evaluating pore formation at different laser-microbeam parameters. DMEM and fetal bovine serum were purchased from Lonza (Maryland). Trypsin was purchased from Mediatech (Manassas, Virginia). All other reagents were purchased from Fisher Scientific, except those specifically mentioned.

2.2 Goldfish Retina Explant

The goldfish retina was extracted as described in earlier studies¹² with modifications, approved by local animal care committee. Adult goldfish (*Carassius auratus*) fish, 5 to 7 cm body length, were housed in a standard glass aquarium at 19° to 21°C. The eyes were removed from goldfish anesthetized after 1 h of dark adaptation to facilitate removal of the pigment epithelium. The retinas were removed and cut into 400 μm square explants on a McIlwain tissue chopper. These were then placed into sterile 35-mm Petri dishes with a 14 mm central hole backed by a glass coverslip (MatTek) previously coated with 0.75 mg/dish poly-D-lysine (Sigma, >300,000 MW in borate buffer, pH 8.3). The explants were oriented ganglion cell side toward the poly-D-lysine, and incubated at room air and temperature in Leibovitz's L15 medium (Sigma) supplemented with 10% fetal bovine serum (Fisher Scientific) and 50 μg/ml gentamicin. Since the fish is poikilothermic, it is easy to maintain the retina *in vitro* in the Petri dishes after transfection, without the need for temperature control.

2.3 Molecules for Injection

For evaluating kinetics of optoporation into mammalian cells, PI was chosen as it does not permeate through the plasma membrane, but stains the nucleus. PI (Invitrogen Inc.) is commonly used for the confirmation of laser-assisted poration into mammalian cells.^{5,13} ChR2 plasmids were chosen for transfection of Goldfish retina explants. ChR2 is emerging as a potential molecular probe for optogenetic stimulation of neurons so as to alter functional activities.¹⁴ Since ChR2 is not fluorescent, EYFP was fused in-frame to the C-terminus of ChR2 by polymerase chain reaction (PCR) for visualization of ChR2 expression in transfected region of retina explant.

2.4 Optical Microinjection Setup

A schematic of the optoporation setup is shown in Fig. 1(a). A femtosecond Ti:Sapphire laser (Newport Spectra-Physics Inc.) beam with a wavelength tuning range from 690 to 1040 nm (rep rate: 80 MHz, pulse width: ~100 fs) was directed toward the sample through either an inverted optical microscope (Nikon Ti-U) or upright optical microscope (Olympus BX 60M). A 100× (NA = 1.3) or 20× (NA = 0.5) objective was used to focus the laser beam to a diffraction limited spot for microinjection into a single cell or a retina, respectively. A dichroic mirror 1 (DM1) was used to combine the laser beam and the beam from the excitation source. The dichroic mirror 2 (DM2) reflects the excitation lamp light and transmits the emitted fluorescence to the CCD. The emission filter (Em) blocked the back-reflected fluorescence excitation and laser beam. Bright field and fluorescence images were captured using a cooled CCD camera and processed using IMAGEJ Software. The number of femtosecond pulses at each point of irradiation was controlled by the width of the microsecond pulses created by a mechanical shutter (S, Uniblitz Inc.). The power of the laser microbeam was varied by controlling the angle of orientation of the polarizer (P). The laser beam power at the sample plane of the 20× objective was measured directly by using a power meter (PM100D, Thorlabs

Inc.). The beam power after the 100 \times objective was calculated by multiplying the transmission factor of the microscope objective (0.60) with the power measured at the back aperture of the objective. The XYZ-scanning of the region of interest in the sample, to be irradiated by the femtosecond laser microbeam, was achieved by controlling the motorized stage movement. The distance between two focused spots, and thus the number of spots in the region of interest (to be transfected), could be varied by moving the stage at different scanning speeds. Further, this can be achieved by a change in the OFF-time between shutter macropulses, for a constant speed of the stage.

2.5 Immunostaining

The retina explant was fixed in 4% paraformaldehyde in 0.1 M phosphate buffer (PBS, pH 7.4), at 4°C for 15 min. Tissue was washed 3 \times 15 min in rinsing buffer (PBS with 5% glucose, pH 7.4, 0.15 CaCl₂ mm, 0.02% Na-azide) and blocked for 20 min with 5% normal goat serum albumin in 0.1 M PBS/0.3% Triton X-100. Explants were incubated overnight in anti-YFP (1:500). Following 3 to 10 min in PBS, sections were blocked with 5% NGS for 20 min, incubated in secondary antibody FITC (1:1000) for 35 min at 37°C, rinsed 3 to 10 min in PBS, and visualized on a microscope. DAPI was used for 10 min at 37°C as a nuclear stain.

2.6 Fluorescence Microscopy

For microinjection experiments in cell culture, the monolayer cells on a Petri dish were incubated with PI (50 μ g/mL, Invitrogen) at 37°C and viewed under a fluorescence microscope (Nikon Ti-U) with 100 \times oil-immersion objective (NA 1.30). Images were collected with a cooled CCD camera with TSVIEW Software (Tucsen Imaging Technology Co., Ltd.). Transgene-expressing neuronal cells in retina explant were identified by visualizing the native EYFP fluorescence (before immunostaining) or YFP-antibody fluorescence with 488 nm laser excitation in a Zeiss LSM 510 META microscope.

2.7 Data Analysis

For analysis of propidium iodide inclusion into a cell, Fick's laws of diffusion, $C - C_0 = D(dC/dt)$ was used, where C is the concentration of fluorescent dye at any instantaneous time, C_0 is maximum concentration of the dye in cells, and D being the diffusion coefficient. Thus the increase in fluorescence intensity could be fitted to a single exponential function as follows: $C/C_0 = 1 - e^{-(t-t_0)/\tau}$, where C/C_0 is the normalized concentration of the fluorescent dye at time t , t_0 being the initial time of dye influx with τ as the rise-time constant.

3 Results and Discussion

3.1 PI is Introduced into the Cell Through Localized Pore Formation

Figure 1 shows red blood cells before [Fig. 1(b)] and after [Fig. 1(c)] laser microbeam irradiation for exposure time of 30 ms, at average power of 16 mW (individual femtosecond pulse energy of 0.2 nJ, repetition rate: 80 MHz), at the focal plane. Array of holes made in RBCs by the NIR femtosecond

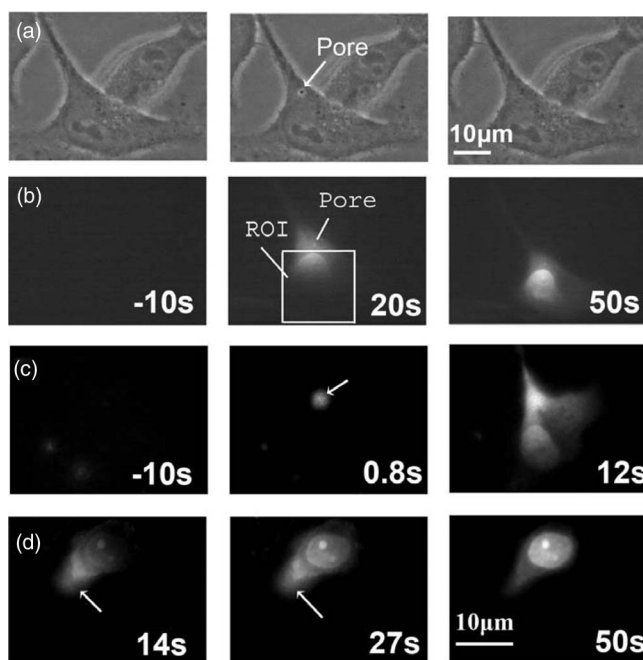


Fig. 2 Time lapse images of laser-assisted microinjection of PI into cells through the arrow-marked pore. (a) Bright field images a HT1080 cell before (left), during (middle), and after (right) laser micro-irradiation. (b) Time-lapse fluorescence images of cell-1 in (a). Time-lapse fluorescence images of microinjection of PI into cell-2 (c) and cell-3 (d).

laser microbeam can be seen in Fig. 1(c). It may be noted that the pore sizes are determined by the diffraction limited spot (radius = 375 nm for 100 \times objective and 975 nm). From phase contrast imaging and atomic force microscopy,¹⁵ the pore sizes are found to match this theoretical limit. For optoporation in mammalian cells, laser power was slowly tuned until no long-term morphological changes were visually observed. Figure 2 shows injection of PI through the arrow-marked pore in three different cells [Figs. 2(b)–2(d)], formed by the femtosecond laser microbeam (pulse energy: 0.2 nJ, exposure time: 20 ms) after 20 s of pore formation in a targeted HT1080 cell. Even after sealing the pore [last panel of Figs. 1(b)–1(d)], distinct fluorescence at the site of pore formation [arrow marked in middle panels of Figs. 1(b)–1(d)] on the membrane was observed. Further, PI was found to stain the nucleus from the site of injection and propagate through the nucleus by diffusion as shown in time lapse series [panels in Figs. 1(b)–1(d)]. This confirms the fact that PI is injected via the pore formed by an ultrafast laser microbeam



Fig. 3 Fluorescence in nucleoli is higher than that of the nucleus distinct spatial localization pattern in nucleus. (a) Bright field image of HIBEC cell. (b) Fluorescent field before optoporation. (c) Fluorescence observed after microinjection. All images are in the same magnification. Scale bar: 10 μ m.

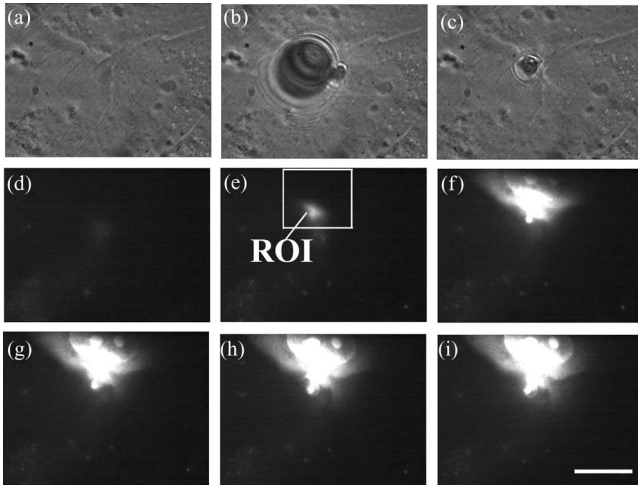


Fig. 4 Time lapse images of laser-assisted microinjection of PI into HIBEC cells with bubble formation. Bright field before (a) and during [(b), (c)] bubble formation. (d) Fluorescence image before optoporation. Fluorescence observed after PI injection at 270 s (e), 290 s (f), 300 s (g), 310 s (h), and 320 s (i). All images are in the same magnification. Scale bar: 10 μm .

and other parts of the cell membrane are intact subsequent to laser irradiation.

3.2 Distinct Spatial Localization Pattern in Nucleus

After diffusion of PI dye over the whole nucleus, the dye seemed to be localized in a distinct spatial pattern with higher fluorescence in the nucleolus. As shown in Figs. 2(b)–2(d), although PI diffused through the part of nucleus close to the pore, fluorescence shows much higher intensity in nucleolus than the other part of the nucleus at similar distances from the pore [Figs. 2(b)–2(d)]. Figure 3 shows a similar effect in an optoporated HIBEC cell. After 2 min of optoporation, fluorescence in nucleoli [Fig. 3(c)] is higher than that of the nucleus. These results are intriguing owing to the fact that PI binds to both nucleic acids by intercalating between the bases with little or no sequence preference.¹⁶ One hypothesis is that the binding affinity of PI to nucleolar content is higher or at least there is higher density of nucleic acids in nucleolus.

3.3 Ultrafast Laser Assisted Cellular Poration via Bubble Formation

Figure 4 shows optoporation in one representative cell subsequent to bubble formation in extracellular medium caused by a longer (60 ms) exposure of laser irradiation and a higher (80 mW) average power (1 nJ/pulse, 80 MHz). The bubble collapsed approximately after 42 s. PI fluorescence in the cell could be observed only after ~ 4 min of bubble formation, indicating the fact that although a larger part of the cell membrane might have stretched, the pore sizes are significantly smaller than direct hole-formation (Sec. 3.2). Further, kinetics of hole-formation and resealing induced by extracellular bubble and direct poration can be very different. It may be noted that no significant rise in PI fluorescence was observed in the encircled cell even up to 6 min, as compared to the cell (marked by a rectangle). This can be attributed to the distance of the two cells being different from the center of the bubble. Microinjection by bubble formation may also depend on the size of the bubble.

To compare the efficiency of PI injection of the two methods (direct poration versus bubble formation), the increase in fluorescence intensity was fitted to a single exponential function. For this comparison, we evaluated direct membrane pore formation versus bubble formation at a distance of 5 to 8 μm for bubble diameter of 8 to 12 μm . As shown in Fig. 5, the initiation time of PI entry for direct pore formation is 13.7 s, much earlier than the initiation entry time in the case of bubble formation (263 s). Moreover, the time constant of poration by a bubble is much higher (56 ± 11 s, $n = 3$) than that of the pore induced directly by a laser microbeam (20 ± 11 s, $n = 3$). For the estimation of standard deviations of the rise-time constants, individual graphs (starting from different injection time points) are fitted and rise-time constants were estimated.

The above results suggest that the influx of PI through pore formed by direct laser microirradiation is much faster than microinjection achieved by bubble formation. Besides varying (local) membrane fragility, the large variation of initiation time and rise-time constants in the case of direct pore formation can be attributed to varying distance of the site of injection from the nucleus. However, in the case of indirect (bubble) poration, the size (8 to 12 μm) and distance (5 to 8 μm) of the bubble from the membrane is expected to influence the initiation of injection time along with the rise time constant.

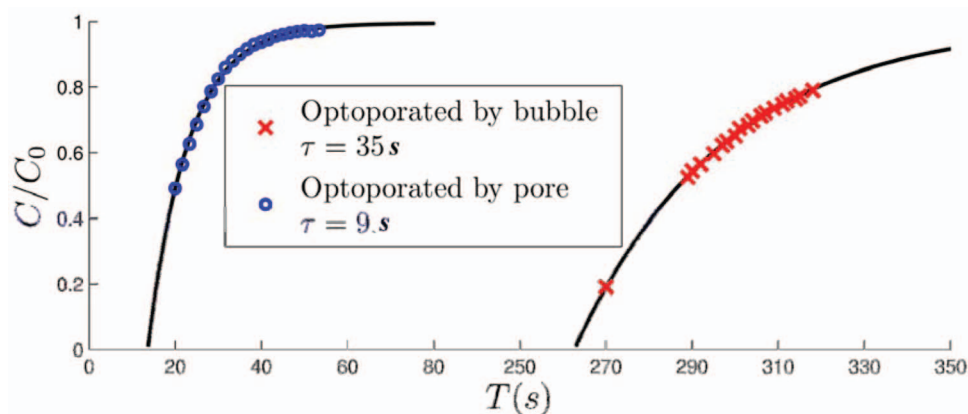


Fig. 5 Single exponential fitting of increase of PI concentration (indicated by rise in fluorescence intensity) in cells after optoporation by direct pore formation versus bubble formation. C : concentration of PI at time t . C_0 : concentration at maximum time.

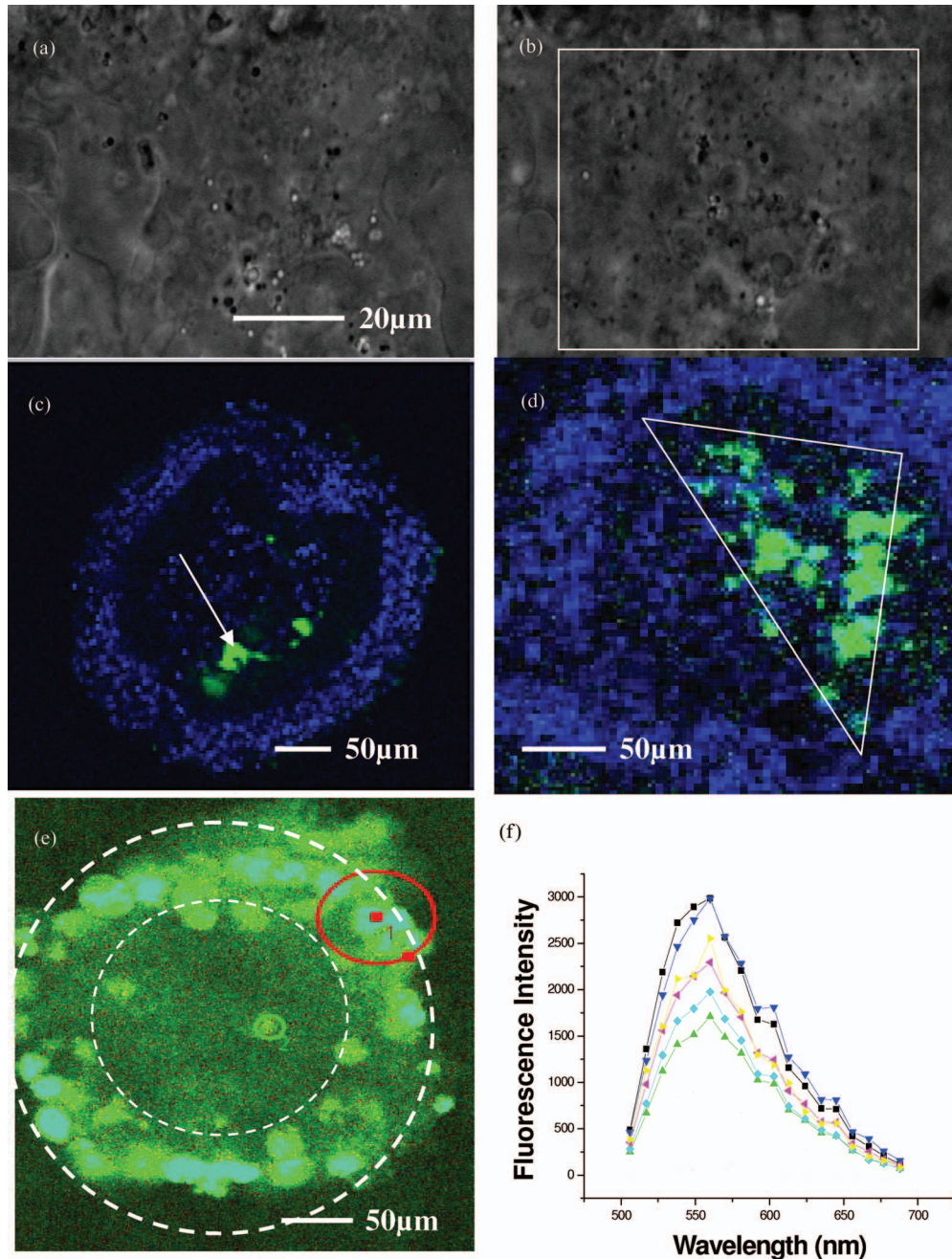


Fig. 6 Optoporation of ChR2 gene into targeted area of goldfish retina. (a) Retina explant; (b) array of dark spots created after patterned irradiation with ultrafast laser microbeam; (c) highly-localized laser transfection of retina explant, immunostained for YFP and co-stained nucleus with DAPI; (d) triangular region transfected with ChR2-YFP by patterned NIR fs laser microbeam; (e) fluorescence spectral imaging (true color) of the peripherally transfected (region between concentric circles) retina explant; (f) fluorescence spectrum from arbitrary locations along the periphery of transfected retina.

3.4 Optoporation of ChR2 Gene into Targeted Area of Retina

ChR2 is a type of light-gated ion channel isolated from the green algae *Chlamydomonas reinhardtii*.¹⁴ It can be activated by blue light and conduct cation ions. The highly-efficient photoactivation property of ChR2 makes it an effective tool for neuronal stimulation¹⁷ and intervention for retinal degenerative diseases such as retinitis pigmentosa (RP)^{18,19} and macular degeneration. In RP, since the photoreceptors are degenerated, the most logical target would be retinal ganglion cells,¹⁹ although photo-

sensitization of bipolar cells¹⁸ have also shown great promise. The delivery of ChR2, especially with promoter targeting to specific type of neurons, is of great importance in optogenetics. While a viral method can deliver optogenetic plasmids, spatially-targeted delivery at a single cell level is not possible. Therefore, for injection of ChR2-YFP plasmids into targeted retinal neurons in the explant [Fig. 6(a)], an array of holes (1 per 3 µm) were made in the retina in the region of interest [marked by a rectangle, Fig. 6(b)] by the NIR femtosecond laser microbeam (0.2 nJ/pulse, 10 ms). For these experiments, retinal ganglion

cells were targeted as they were proximal to the laser source. The array of dark spots (sealed holes) created after patterned irradiation with an ultrafast laser microbeam is seen in Fig. 6(b). The multiphoton process, as it exists in the femtosecond microbeam, ensures localized perforation in a specific layer.

Highly-localized laser transfection of ChR2-YFP in retina explant, immunostained for YFP and co-stained nucleus with DAPI, is shown in Fig. 6(c). Figure 6(d) shows the triangular region of the explant being transfected with ChR2-YFP by a patterned NIR femtosecond laser microbeam. Figure 6(e) shows fluorescence spectral imaging (LSM META 510) of peripherally transfected (region between concentric circles) retinal cells in the explant. The fluorescence spectra from arbitrary points in the periphery [Fig. 6(f)] confirmed the YFP expression in targeted retinal tissue. Optoporation of the ChR2 gene into a targeted spatial location of the retina is thus demonstrated with an ultrafast laser microbeam, which may be extended for *in vivo* application in order to restore peripheral vision lost in RP.¹⁹ However, it is important to further investigate the potential injury of this method on neuronal cells.

4 Conclusions

Kinetics of fluorescence dye injection into vital cells by NIR femtosecond laser-assisted perforation was evaluated using two different approaches, i. localized pore formation and ii. extracellular bubble formation. The injection rate (indicated by an increase in fluorescence) by bubble formation was found to be much slower than direct pore formation. A distinct spatial localization pattern with higher PI fluorescence in the nucleoli as compared to other parts of the nucleus was observed, which may indicate significant binding affinity of PI to nucleolar content. Laser assisted delivery of exogenous material into a specific two-dimensional area in the neuronal tissue, such as the retina, as demonstrated in these (preliminary) experiments, will help to understand the functioning of neuronal circuitry of normal and degenerated retina. For confirming functional aspects of ChR2 expression, the transfected retina needs to be examined using electrophysiology subsequent to light stimulation.^{17–19} Further work on the use of long working-distance optics and optimization of laser irradiation parameters (wavelength, focused spot size, exposure, etc.) need to be carried out in order to achieve efficient *in vivo* transfection.

Acknowledgments

The authors would like to thank Professor David Gilley, Indiana University-School of Medicine for the HT1080 cells and Professor Eric Gershwin, University of California Davis-School of Medicine for the HIBEC cells.

References

1. W. Tao, J. Wilkinson, E. J. Stanbridge, and M. W. Berns, "Direct gene transfer into human cultured cells facilitated by laser micropuncture of the cell membrane," *Proc. Natl. Acad. Sci. U.S.A.* **84**(12), 4180–4184 (1987).
2. H. Schneckenburger, A. Hendinger, R. Sailer, W. S. Strauss, and M. Schmitt, "Laser-assisted optoporation of single cells," *J. Biomed. Opt.* **7**(3), 410–416 (2002).
3. G. Palumbo, M. Caruso, E. Crescenzi, M. F. Tecce, G. Roberti, and A. Colasanti, "Targeted gene transfer in eucaryotic cells by dye-assisted laser optoporation," *J. Photochem. Photobiol. B* **36**(1), 41–46 (1996).
4. J. S. Soughayer, T. Krasieva, S. C. Jacobson, J. M. Ramsey, B. J. Tromberg, and N. L. Allbritton, "Characterization of cellular optoporation with distance," *Anal. Chem.* **72**(6), 1342–1347 (2000).
5. S. K. Mohanty, M. Sharma, and P. K. Gupta, "Laser-assisted microinjection into targeted animal cells" *Biotechnol. Lett.* **25**(11), 895–899 (2003).
6. Y. Hosokawa, S. Iguchi, R. Yasukuni, Y. Hiraki, C. Shukunami, and H. Masuhara, "Gene delivery process in a single animal cell after femtosecond laser microinjection," *Appl. Surf. Sci.* **255**(24), 9880–9884 (2009).
7. F. Stracke, I. Rieman, and K. König, "Optical nanoinjection of macromolecules into vital cells," *J. Photochem. Photobiol. B: Biol.* **81**(3), 136–142 (2005).
8. H. Schinkel, P. Jacobs, S. Schillberg, and M. Wehner, "Infrared picosecond laser for perforation of single plant cells," *Biotechnol. Bioeng.* **99**(1), 244–248 (2008).
9. U. K. Tirlapur and K. König, "Targeted transfection by femtosecond laser," *Nature* **418**(6895), 290–291 (2002).
10. G. Paltauf and P. E. Dyer, "Photomechanical processes and effects in ablation," *Chem. Rev.* **103**(2), 487–518 (2003).
11. A. Vogel, J. Noack, G. Hüttman, and G. Paltauf, "Mechanisms of femtosecond laser nanosurgery of cells and tissues," *Appl. Phys. B* **81**(8), 1015–1047 (2005).
12. S. Zimov and S. Yazulla, "Vanilloid receptor 1 (TRPV1/VR1) colocalizes with fatty acid amide hydrolase (FAAH) in retinal amacrine cells," *Vis. Neurosci.* **24**(4), 581–591 (2007).
13. L. Rienzi, F. Ubaldi, F. Martinez, M. G. Minasi, M. Iacobelli, S. Ferrero, J. Tesarik, and E. Greco, "Clinical application of laser-assisted ICSI: a pilot study," *European J. Obstetrics & Gynecol. Reprod. Biol.* **115**(Supplement 1), S77–S79 (2004).
14. G. Nagel, T. Szellas, W. Huhn, S. Kateriya, N. Adeishvili, P. Berthold, D. Ollig, P. Hegemann, and E. Bamberg, "Channelrhodopsin-2, a directly light-gated cation-selective membrane channel," *Proc. Nat. Acad. Sci. U.S.A.* **100**(24), 13940–13945 (2003).
15. N. Ingle and S. K. Mohanty, "Live atomic force microscopy imaging of laser microbeam assisted cellular microsurgery," *Proc. SPIE* **7902**, 79020L (2011).
16. M. J. Waring, "Complex formation between ethidium bromide and nucleic acids," *J. Mol. Biol.* **13**(1), 269–282 (1965).
17. F. Zhang, L.-P. Wang, E. S. Boyden, and K. Deisseroth, "Channelrhodopsin-2 and optical control of excitable cells," *Nature Meth.* **3**(10), 785–792 (2006).
18. P. S. Lagali, D. Balya, G. B. Awatramani, T. A. Münch, D. S. Kim, V. Busskamp, C. L. Cepko, and B. Roska, "Light-activated channels targeted to ON bipolar cells restore visual function in retinal degeneration," *Nat. Neurosci.* **11**(6), 667–675 (2008).
19. S. Shivalingaiah, L. Gu, and S. K. Mohanty, "Correlation of spatial intensity distribution of light reaching the retina and restoration of vision by optogenetic stimulation," *Proc. SPIE* **7885**, 78851Y (2011).